Eigenmodes of an Asymmetric Cylindrical Confocal Laser Resonator with a Single Output-Coupling Aperture

By D. E. McCUMBER

(Manuscript received February 24, 1969)

Previous calculations of the low-loss modes of a symmetric cylindrical confocal laser resonator have been extended to the asymmetric case. Diffraction losses are governed by the geometric-mean Fresnel number $\mathrm{N_m}$ *of the two end mirrors and, in the system we consider, by the Fresnel number* $\mathrm{N_o}$ *of an output coupling aperture in one of the mirrors. Loss factors and mirror field distributions have been calculated numerically for different* $\mathrm{N_o}$ *for* $\mathrm{N_m}$ *in the range* $0.6 \leqq \mathrm{N_m} \leqq 2$.

I. INTRODUCTION

In a previous paper[1] we described the diffraction losses and the field distributions at the reflectors of the low-loss modes of a symmetric cylindrical confocal resonator for Fresnel numbers $0.6 \leqq N_m \leqq 2$. We considered the effect of output-coupling apertures in the reflectors but we assumed that both reflectors were identical, each with the same output aperture and the same maximum radius. In this paper we again consider the cylindrical confocal geometry, but we do not require identical reflectors and, in particular, we assume that only one reflector is pierced by an output-coupling aperture, as in the coupling scheme proposed by Patel and others.[2]

Figure 1 shows an axial section of the confocal resonator in question. The cavity is bounded at its two ends by confocal spherical mirrors (more exactly, confocal paraboloids[3]). The first mirror is perfectly reflecting over the annular region $0 \leqq a_{1o} \leqq \rho \leqq a_{1m}$, the second over the circular section $0 \leqq \rho \leqq a_{2m}$. The maximum radii ($a_{1m}$, a_{2m}) are both much less than the mirror separation b.

Expressions for the eigenvalues and eigenfunctions of asymmetric rectangular confocal resonators with output coupling slits have been

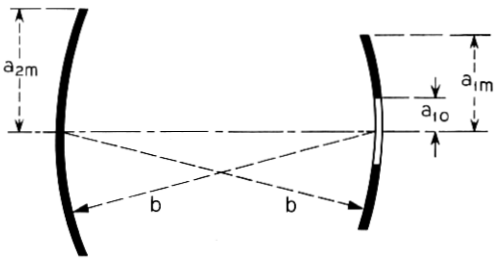

Fig. 1 — Axial section of cylindrical confocal laser cavity. The cavity is bounded at its two ends by confocal spherical mirrors with radius of curvature b. One mirror is perfectly reflecting over the annular region $0 \leqq a_{1o} \leqq \rho \leqq a_{1m}$, the other over the circular section $0 \leqq \rho \leqq a_{2m}$. Both a_{1m} and a_{2m} are much less than b.

derived by Boyd and Kogelnik.[4] Properties of symmetric resonators without coupling apertures are summarized with an extensive list of references in the review article by Kogelnik.[5] Equivalence relations relating asymmetric and symmetric resonators with circular mirrors have been derived by Gordon and Kogelnik.[6]

Our analysis of the resonator of Fig. 1 closely parallels that of the symmetric resonator.[1] Assuming that all dimensions are large compared with the optical wavelength λ, we again use a scalar formulation of Huygens' principle.[3–5] For the cylindrical confocal geometry the field amplitude at reflector j, $j = 1$ or 2, for a typical mode can be written in the form

$$F_{lp}^{(j)}(\rho, \varphi) = f_{lp}^{(j)}(\rho) \exp(-il\varphi), \tag{1}$$

where (ρ, φ) are radial and angular coordinates in a plane perpendicular to the resonator axis and where (l, p) are angular and radial quantum integers (transverse quantum numbers). For this asymmetric system with nonidentical mirrors, we cannot require for an eigenmode that the field amplitude distribution $F_{lp}^{(j)}(\rho, \varphi)$ at one mirror be a constant multiple of that at the other. Rather, we must require for eigenmodes that after a round-trip transit of the resonator the field amplitude at one mirror be a constant multiple of the initial field amplitude at the same mirror. This more elaborate self-reproducing requirement together with Huygens' principle gives the following pair of simultaneous integral equations which must be satisfied by the radial eigenfunctions $f_{lp}^{(j)}(\rho)$ and eigenvalues $\kappa_{lp}^{(j)}$ [compare equation (2) of Ref. 1].

$$\kappa_{lp}^{(2)} f_{lp}^{(2)}(\rho_2) = \frac{2\pi}{b\lambda} \int_{a_{1o}}^{a_{1m}} d\rho_1 \ \rho_1 J_l(2\pi\rho_2\rho_1/b\lambda) f_{lp}^{(1)}(\rho_1), \tag{2a}$$

$$\kappa_{lp}^{(1)} f_{lp}^{(1)}(\rho_1) = \frac{2\pi}{b\lambda} \int_o^{a_{2m}} d\rho_2 \, \rho_2 J_l(2\pi\rho_1\rho_2/b\lambda) f_{lp}^{(2)}(\rho_2). \tag{2b}$$

$J_l(z)$ is the Bessel function of order $|l|$. The loss factor is

$$\alpha_{lp} = 1 - |\kappa_{lp}^{(1)}\kappa_{lp}^{(2)}|, \tag{3}$$

which is the fractional energy of a mode lost per reflection (or during the one-way transit time b/c, where c is the velocity of light in the resonator).[5] The phase of the eigenvalue product $\kappa_{lp}^{(1)}\kappa_{lp}^{(2)}$ determines the resonant wavelength:

$$\text{resonant } \lambda = 4\pi b/[(l+1)\pi - \operatorname{Arg} \kappa_{lp}^{(1)}\kappa_{lp}^{(2)} - 2\pi n], \tag{4}$$

where n is an arbitrary integer (longitudinal quantum number).

It is useful to introduce the mirror Fresnel numbers

$$N_m^{(1)} = a_{1m}^2/\lambda b, \qquad N_m^{(2)} = a_{2m}^2/\lambda b, \tag{5a}$$

and their geometric mean

$$N_m \equiv [N_m^{(1)} N_m^{(2)}]^{\frac{1}{2}} = a_{1m}a_{2m}/\lambda b. \tag{5b}$$

In place of the variables ρ_j and the functions $f_{lp}^{(j)}(\rho_j)$ in equations (2), we introduce new variables

$$r_j = r_m \rho_j / a_{jm} \tag{6a}$$

and functions

$$g_{lp}^{(j)}(r_j) = f_{lp}^{(j)}(r_j a_{jm}/r_m), \tag{6b}$$

where $r_m^2 = N_m$. We characterize the size of the radius-a_{1o} hole in the first mirror by the Fresnel number

$$N_o \equiv r_o^2 = (a_{1o}/a_{1m})^2 N_m = a_{1o}^2 a_{2m}/\lambda b a_{1m}. \tag{7}$$

With no significant loss of generality we can define the functions $f_{lp}^{(j)}(\rho_j)$ such that

$$a_{2m}\kappa_{lp}^{(2)}/a_{1m} = a_{1m}\kappa_{lp}^{(1)}/a_{2m} = \kappa_{lp} \tag{8}$$

and

$$\delta_{pq} = 2\pi \int_{r_o}^{r_m} dr_1 \, r_1 g_{lp}^{(1)}(r_1) g_{lq}^{(1)}(r_1), \tag{9a}$$

$$\delta_{pq} = 2\pi \int_o^{r_m} dr_2 \, r_2 g_{lp}^{(2)}(r_2) g_{lq}^{(2)}(r_2). \tag{9b}$$

With this notation the eigenvalue equations (2) become

$$\kappa_{lp} g_{lp}^{(2)}(r_2) = 2\pi \int_{r_o}^{r_m} dr_1\, r_1 J_l(2\pi r_2 r_1) g_{lp}^{(1)}(r_1), \tag{10a}$$

$$\kappa_{lp} g_{lp}^{(1)}(r_1) = 2\pi \int_{o}^{r_m} dr_2\, r_2 J_l(2\pi r_1 r_2) g_{lp}^{(2)}(r_2). \tag{10b}$$

Equation (3) simplifies to

$$\alpha_{lp} = 1 - |\kappa_{lp}|^2, \tag{11}$$

which depends upon the parameters (a_{1o}, a_{1m}, a_{2m}, b, λ) only through the Fresnel numbers $N_m = r_m^2$ and $N_o = r_o^2$. In what follows we describe how the loss factor α_{lp} and the amplitudes $g_{lp}^{(i)}(r)$ change with N_o for N_m in the interval $0.6 \leqq N_m \leqq 2$. Solutions for $N_o = 0$ are described elsewhere.[1,3,7–9]

Our numerical method is similar to that previously described for the symmetric resonator.[1] We expand the Bessel-function kernels in equation (10) as power series, truncate the series after a finite number $M = \max(10\, N_m + 1, 10)$ of terms, and reduce the integral equations (10) to M-dimensional matrix equations which are solved numerically with standard matrix routines. [The reduction of equation (10) to matrix form is described in the Appendix.] The merits of this technique remain as described before.[1]

II. ANALYTIC METHODS FOR SMALL N_o

The eigenvalues κ_{lp} and field amplitudes $g_{lp}(r)$ for $N_o = 0$ are described elsewhere.[1,3,7–9] The loss factor $\alpha_{lp} = 1 - |\kappa_{lp}|^2$ for the four lowest-loss modes (compare with Fig. 2 of Ref. 1) are tabulated for $0.6 \leqq N_m \leqq 2$ in Table I. For $l = 0$, the field amplitude $g_{lp}(r)$ at $r = 0$ is finite; for $l \neq 0$, it vanishes as $r^{|l|}$. As before, we expect the modes with angular quantum number $l = 0$ to be more sensitive to the coupling aperture ($N_o > 0$) than the $l \neq 0$ modes.[1]

If we use a superscript "0" to lable the eigenvalues and field amplitudes for $N_o = 0$, then for small r, to within corrections of relative order r^2,

$$g_{lp}^0(r) = g_{0p}^0(0) \quad \text{for} \quad l = 0 \tag{12a}$$

$$= c_{lp}^0 r^{|l|} \quad \text{for} \quad l \neq 0, \tag{12b}$$

where coefficients $g_{0p}^0(0)$ are listed in Table II (an expanded version of Table III, Ref. 1) and coefficients c_{lp}^0 in Table III. The forms (12) are

TABLE I—LOSS FACTOR α_{lp} FOR $N_o = 0$

N_m	$\alpha_{00}{}^0$	$\alpha_{01}{}^0$	$\alpha_{10}{}^0$	$\alpha_{20}{}^0$
0.6	3.614×10^{-2}	0.7931	0.2724	0.6679
0.7	1.301×10^{-2}	0.6131	0.1371	0.4712
0.8	4.448×10^{-3}	0.4131	6.103×10^{-2}	0.2900
0.9	1.471×10^{-3}	0.2411	2.477×10^{-2}	0.1563
1.0	4.759×10^{-4}	0.1233	9.417×10^{-3}	7.505×10^{-2}
1.1	1.515×10^{-4}	5.651×10^{-2}	3.424×10^{-3}	3.285×10^{-2}
1.2	4.767×10^{-5}	2.382×10^{-2}	1.206×10^{-3}	1.343×10^{-2}
1.3	1.485×10^{-5}	9.462×10^{-3}	4.151×10^{-4}	5.225×10^{-3}
1.4	4.59×10^{-6}	3.601×10^{-3}	1.403×10^{-4}	1.961×10^{-3}
1.5	1.41×10^{-6}	1.328×10^{-3}	4.674×10^{-5}	7.164×10^{-4}
1.6	4.3×10^{-7}	4.78×10^{-4}	1.539×10^{-5}	2.561×10^{-4}
1.7	1.3×10^{-7}	1.69×10^{-4}	5.01×10^{-6}	9.000×10^{-5}
1.8	4×10^{-8}	5.89×10^{-5}	1.62×10^{-6}	3.116×10^{-5}
1.9	1×10^{-8}	2.02×10^{-5}	5.2×10^{-7}	1.066×10^{-5}
2.0	4×10^{-9}	6.86×10^{-6}	1.7×10^{-7}	3.60×10^{-6}

useful for estimating the perturbations induced by a small finite N_o. To first order, the perturbed field amplitudes are

$$g_{lp}^{(1)}(r) = g_{lp}^0(r)\left\{1 + \pi \int_o^{r_o} dr_1\, r_1[g_{lp}^0(r_1)]^2\right\}$$

$$- \sum_{q \neq p}{}' g_{lq}^0(r) \frac{(\kappa_{lq}^0)^2}{(\kappa_{lp}^0)^2 - (\kappa_{lq}^0)^2} 2\pi \int_o^{r_o} dr_1\, r_1 g_{lq}^0(r_1) g_{lp}^0(r_1), \qquad (13a)$$

TABLE II—FIELD AMPLITUDE AT $r = 0$ FOR $l = 0$ MODES WITH $N_o = 0$

N_m	$g_{00}{}^0(0)$	$g_{01}{}^0(0)$	$g_{02}{}^0(0)$
0.6	1.2770	1.2251	1.6159
0.7	1.3021	1.1541	1.4851
0.8	1.3213	1.1254	1.3735
0.9	1.3354	1.1286	1.2760
1.0	1.3457	1.1511	1.1930
1.1	1.3536	1.1807	1.1291
1.2	1.3597	1.2093	1.0890
1.3	1.3647	1.2336	1.0742
1.4	1.3688	1.2532	1.0812
1.5	1.3723	1.2688	1.1025
1.6	1.3752	1.2814	1.1302
1.7	1.3778	1.2918	1.1580
1.8	1.3800	1.3006	1.1826
1.9	1.3820	1.3081	1.2033
2.0	1.3838	1.3146	1.2203
∞	$\sqrt{2} = 1.4142$	1.4142	1.4142

TABLE III—FIELD-AMPLITUDE COEFFICIENT FOR $l \neq 0$ MODES AT $r = 0$ FOR $N_o = 0$

N_m	$c_{10}{}^0$	$c_{11}{}^0$	$c_{20}{}^0$
0.6	2.6428	4.4649	3.9948
0.7	2.7222	4.0086	3.9131
0.8	2.8269	3.7024	3.9979
0.9	2.9266	3.5247	4.1770
1.0	3.0094	3.4618	4.3917
1.1	3.0746	3.4932	4.5999
1.2	3.1255	3.5889	4.7809
1.3	3.1659	3.7148	4.9305
1.4	3.1988	3.8431	5.0526
1.5	3.2260	3.9580	5.1531
1.6	3.2491	4.0549	5.2371
1.7	3.2690	4.1351	5.3087
1.8	3.2862	4.2017	5.3704
1.9	3.3014	4.2578	5.4244
2.0	3.3148	4.3059	5.4721
∞	$2\pi^{1/2} = 3.5449$	$2^{3/2}\pi^{1/2} = 5.0133$	$2\pi = 6.2832$

$$g_{lp}^{(2)}(r) = g_{lp}^{0}(r) - \sum_{q \neq p}{}' g_{lq}^{0}(r) \frac{\kappa_{lp}^{0}\kappa_{lq}^{0}}{(\kappa_{lp}^{0})^2 - (\kappa_{lq}^{0})^2} \cdot 2\pi \int_{o}^{r_o} dr_1\, r_1 g_{lq}^{0}(r_1) g_{lp}^{0}(r_1). \tag{13b}$$

To second order, the loss factor is

$$\alpha_{lp} = \alpha_{lp}^{0} + (1 - \alpha_{lp}^{0})2\pi \int_{0}^{r_o} dr_1\, r_1 [g_{lp}^{0}(r_1)]^2 - \sum_{q \neq p}{}' \frac{(1 - \alpha_{lq}^{0})(1 - \alpha_{lp}^{0})}{\alpha_{lq}^{0} - \alpha_{lp}^{0}} \left[2\pi \int_{o}^{r_o} dr_1\, r_1 g_{lq}^{0}(r_1) g_{lp}^{0}(r_1) \right]^2. \tag{14}$$

In deriving (14), we used the fact that for the cylindrical confocal geometry the eigenvalues κ_{lp} are real and $\kappa_{lp}^2 = |\kappa_{lp}|^2$.

The last terms in (13) and (14) describe mode mixing by the aperture. The amount of mixing depends upon the separation of the eigenvalues as well as upon the strength of the perturbation. Degenerate or nearly degenerate modes are much more sensitively coupled than are modes with greatly different losses. In the symmetric resonator the even-p and odd-p modes of a particular angular quantum number l do not mix; such modes do mix in the asymmetric geometry.[1]

For N_o sufficiently small, we can neglect the second-order or mode-mixing term in (14). If we use the small-r approximations (12) in the remaining integral, we find for $l = 0$ that

$$\alpha_{0p} = \alpha_{0p}^{0} + (1 - \alpha_{0p}^{0})\pi N_0[g_{0p}^{0}(0)]^2 \tag{15a}$$

and for $l \neq 0$ that

$$\alpha_{lp} = \alpha_{lp}^{0} + (1 - \alpha_{lp}^{0})\pi(c_{lp}^{0})^2 N_o^{|l|+1}/(|\, l \,| + 1). \tag{15b}$$

These expressions confirm our previous conjecture that modes with $l = 0$ are more sensitive to aperture loss than are modes with $l \neq 0$.

A quantity of interest in the design of lasers with aperture output coupling is that value N_{oc} of N_o for which the losses of the longitudinal (00) mode equal the losses of the (least lossy) transverse (10) mode.[2] All other things being equal, the laser will operate in the (00) mode for $N_o < N_{oc}$, in the (10) mode for $N_o > N_{oc}$, and in still another mode for larger values of N_o. Using Eqs. (15), we estimate that

$$N_{oc} = (\alpha_{10}^{0} - \alpha_{00}^{0})/\pi(1 - \alpha_{00}^{0})[g_{00}^{0}(0)]^2. \tag{16}$$

III. NUMERICAL RESULTS FOR N_o FINITE

Let us compare estimates based upon the approximate expressions (15) and (16) with accurate numerical results. Using the numerical technique outlined at the end of the introduction and in greater detail in the Appendix, we have computed the loss factor α_{lp} for N_o finite and N_m in the range $0.6 \leqq N_m \leqq 2$. Results for $N_m = 0.8$ and N_o variable are shown in Fig. 2 and similar results for $N_m = 1.6$ in Fig. 3. Results for $N_o = 0.001$ and N_m variable are shown in Fig. 4. These examples were chosen to facilitate comparison with the two-aperture symmetric geometry of Ref. 1. The results are qualitatively similar to those obtained before, except that here odd-p and even-p modes interact whereas before they did not.

Predictions based upon the first-order expressions (15) and Tables I to III are shown as dashed lines in Figs. 2 and 3. The fit to the exact results is good for sufficiently small N_o, but deviations are large for those N_o's for which the interaction between the (l, p) and $(l, p + 1)$ modes is evident as a repulsion in the calculated loss curves.

The critical single-aperture Fresnel number N_{oc} for which the loss factor α_{lp} of the longitudinal (00) mode equals that of the lowest transverse (10) mode is shown as a function of mirror Fresnel number N_m in Fig. 5. This is an important parameter in the design of aperture-

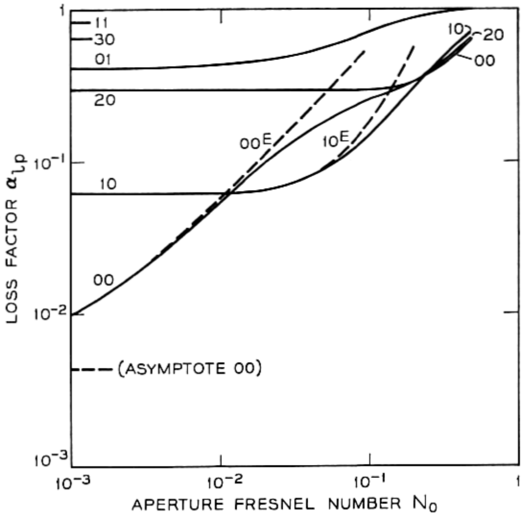

Fig. 2 — Loss factor α_{lp} versus single-aperture Fresnel number N_o for low-loss modes when $N_m = 0.8$. (Compare with Fig. 9 of Ref. 1 for the symmetric two-aperture geometry.) The dashed lines are estimates based on equation (15) and the data from Tables I through III.

out-put-coupled cavities having good mode selection.[2] Also shown in Fig. 5 is the estimate of N_{oc} derived from Eq. (16) and the data from Tables I through III. The agreement is reasonably good, and consistent with what one would expect from the accuracy of the estimates derived from Eqs. (15) in Figs. 2 and 3.

The effect of mode coupling is apparent in the amplitude $g_{lp}^{(i)}(r)$ of the field at the two mirrors. Consider the $l = 0$ modes, which are those most sensitive to finite N_o. The field amplitudes and intensities at the mirrors of the two lowest-loss modes are shown for $N_m = 0.8$ in Figs. 6 and 7 and for $N_m = 1.6$ in Figs. 8 through 11. Figures 6 and 8 show the distributions for $N_o = 0$; they are the same on both mirrors. [Distributions for other (lp) modes are shown for $N_o = 0$ in Ref. 1.] The other figures show how the distributions change for $N_o > 0$. In each figure the dashed lines indicate the field distributions on the mirror pierced by the aperture, the solid lines those on the intact mirror. The radius of the mirrors and the radius of the aperature are indicated on the plots.

One should distinguish two effects apparent in the field plots as N_o increases. First, there is a change in the magnitude of the field amplitude $g_{lp}^{(1)}(r)$ on the pierced mirror. This is a simple renormalization correction implicit in the requirement (9) that the fields be normalized over the reflecting areas of the mirrors. Second, there are changes in the shape of the field distributions on both mirrors. This is a consequence of mode mixing, which becomes appreciable for those N_o's for which significant mode repulsion is apparent in the curves of Figs. 2 and 3. In each case the effect is to reduce the intensity of the less-lossy mode in regions where the mirrors are not reflecting, at the expense of the more lossy of the two interacting modes. This is apparent, for example, in Fig. 9 with $N_m = 1.6$ and $N_o = 0.0001$, for which there is appreciable interaction between the (00) and (01) modes (compare with Fig. 3). The amplitude of the (00) mode at the aperture is decreased below that in Fig. 9; that of the (01) mode is increased. In Fig. 11 with $N_m = 1.6$

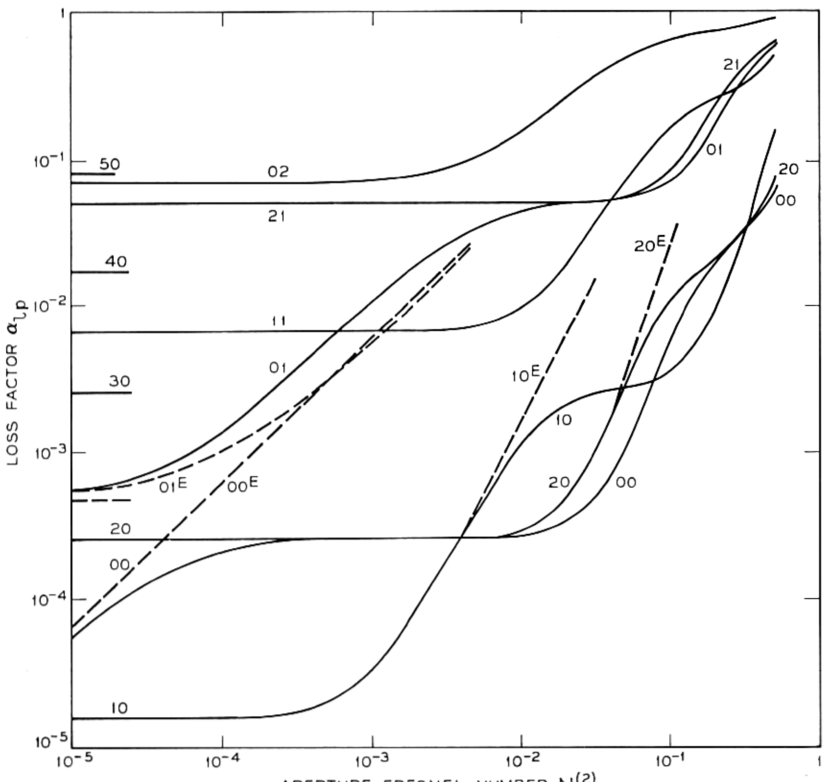

Fig. 3 — Loss factor α_{lp} versus single-aperture Fresnel number N_o for low-loss modes when $N_m = 1.6$. (Compare with Fig. 11 of Ref. 1 for the symmetric two-aperture geometry.) The dashed lines are estimates based on equation (15) and the data from Tables I through III.

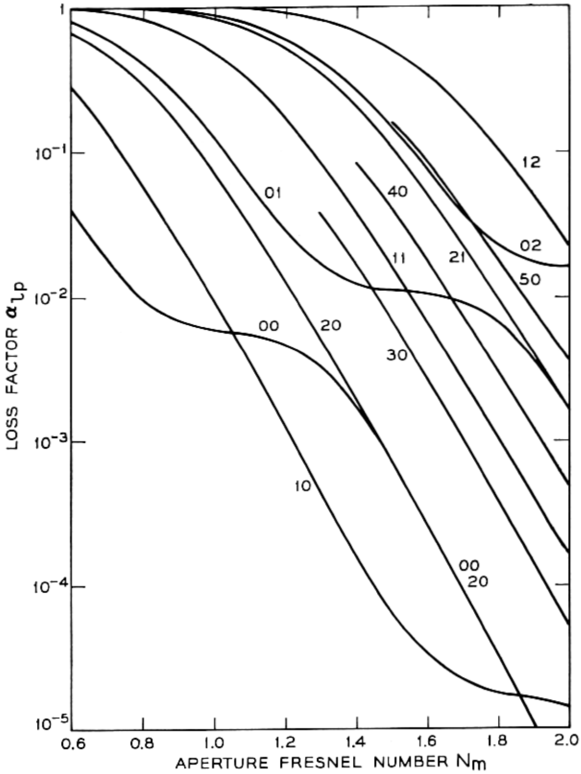

Fig. 4 — Loss factor α_{lp} versus Fresnel number N_m for low-loss modes with N_o fixed at 0.001. (Compare with Fig. 16 of Ref. 1 for the symmetric two-aperture geometry.)

and $N_o = 0.01$, the amplitude of the (01) mode at the aperture is reduced as a consequence of interaction with the (02) mode (Fig. 3).

IV. DISCUSSION

Our previous treatment[1] of a symmetric cylindrical confocal laser cavity is extended here to the asymmetric cylindrical confocal geometry of Fig. 1 and specific numerical values for the loss factor and for the field distributions at the mirrors have been calculated for Fresnel numbers $0.6 \leqq N_m \leqq 2$. The transformations outlined in Section I show that the loss factor of a cavity with different-sized mirrors $(N_m^{(1)} \neq N_m^{(2)})$ equals that of a cavity having two mirrors with the same outer dimensions $[N_m = (N_m^{(1)} N_m^{(2)})^{\frac{1}{2}}]$. The field distributions scale accordingly [see equations (6)]. Similar results also obtain in the rectangular confocal geometry.[4]

For sufficiently small aperture Fresnel numbers N_o the cavity losses associated with a single output coupling aperture can be estimated as in equations (15) from first-order perturbation theory. Just as in the symmetric two-aperture case considered previously, the value of N_o for which such first-order calculations fail decreases rapidly as the Fresnel number N_m increases, because the field distributions distort through mode mixing to minimize the aperture losses in the lowest-loss modes.[1] As before, this distortion occurs at approximately those values of N_o and N_m for which an observer at one reflector, using light of the relevant wavelength and optics limited by the radius $r_m = N_m^{\frac{1}{2}}$, can resolve the aperture of radius $r_o = N_o^{\frac{1}{2}}$ from the other reflector.[1,10]

APPENDIX

Reduction of Integral Equations to Matrix Equations

We express the Bessel-function kernels in power-series form. ($l = |l|$ throughout this appendix.)

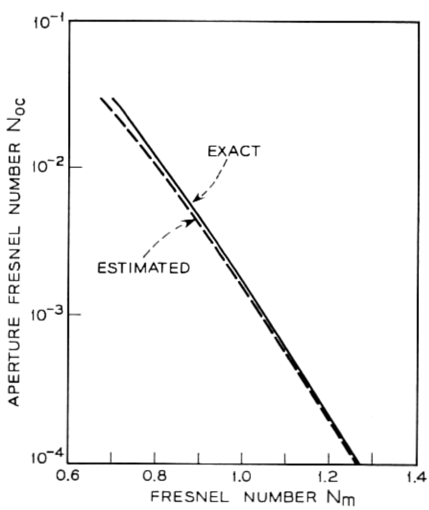

Fig. 5 — Critical single-aperture Fresnel number N_{oc} for which diffraction losses of longitudinal (00) mode equal those of the lowest transverse (10) mode versus Fresnel number N_m. (Compare with Fig. 18 of Ref. 1 for the symmetric two-aperture geometry.) The dashed line is an estimate based on equation (16) and the data from Tables I through III.

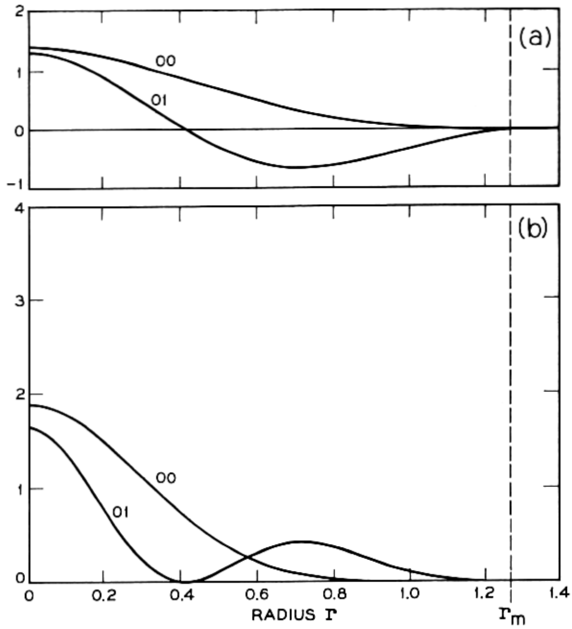

Fig. 6 — (a) Field amplitude $g_{lp}(r)$ and (b) field intensity $|g_{lp}(r)|^2$ for modes $(lp) = (00)$ and (01) with $N_m = 0.8$ and $N_o = 0$. The field distributions are identical on both mirrors.

$$J_l(2\pi r_1 r_2) = (\pi r_1 r_2)^l \sum_{m=1}^{\infty} \frac{(-1)^{m-1}(\pi r_1 r_2)^{2(m-1)}}{(m+l-1)!\,(m-1)!}. \tag{17}$$

Truncating this series after M terms and substituting the result into (10a), we obtain

$$\kappa_{lp} g_{lp}^{(2)}(r_2) = 2\pi \int_{r_o}^{r_m} dr_1\, r_1 \sum_{m-1}^{M} \frac{(-1)^{m-1}(\pi r_1 r_2)^{l+2(m-1)}}{(m+l-1)!\,(m-1)!}\, g_{lp}^{(1)}(r_1) \tag{18a}$$

$$= \left[\frac{(\pi r_2^2)^l}{l!}\right]^{\frac{1}{2}} \sum_{m=1}^{M} \frac{(-1)^{m-1}(\pi r_2^2)^{m-1}}{[(m-1)!\,(m+l-1)!/l!]^{\frac{1}{2}}}\, G_m^{(1)}(l, p), \tag{18b}$$

where

$$G_m^{(1)}(l, p) = \frac{2\pi}{[(m+l-1)!\,(m-1)!]^{\frac{1}{2}}} \int_{r_o}^{r_m} dr_1\, r_1 (\pi r_1^2)^{m-1+l/2} g_{lp}^{(1)}(r_1). \tag{19}$$

Likewise we obtain from (10b)

$$\kappa_{lp} g_{lp}^{(1)}(r_1) = \left[\frac{(\pi r_1^2)^l}{l!}\right]^{\frac{1}{2}} \sum_{m=1}^{M} \frac{(-1)^{m-1}(\pi r_1^2)^{m-1}}{[(m-1)!\,(m+l-1)!/l!]^{\frac{1}{2}}} G_m^{(2)}(l, p), \qquad (20)$$

where

$$G_m^{(2)}(l, p) = \frac{2\pi}{[(m+l-1)!\,(m-1)!]^{\frac{1}{2}}} \int_o^{r_m} dr_2\, r_2 (\pi r_2^2)^{m-1+l/2} g_{lp}^{(2)}(r_2). \quad (21)$$

Substituting the expression (20) for $g_{lp}^{(1)}(r_1)$ into the right hand side of (19) and the expression (18b) for $g_{lp}^{(2)}(r_2)$ into (21), we obtain after simple manipulations

$$\kappa_{lp} G_m^{(1)}(l, p) = \sum_{k=1}^{M} \frac{(-1)^{k-1}[(\pi N_m)^{l+m+k-1} - (\pi N_o)^{l+m+k-1}]}{[(m-1)!\,(m+l-1)!\,(k-1)!\,(k+l-1)!]^{\frac{1}{2}}(l+m+k-1)} G_k^{(2)}(l, p), \qquad (22a)$$

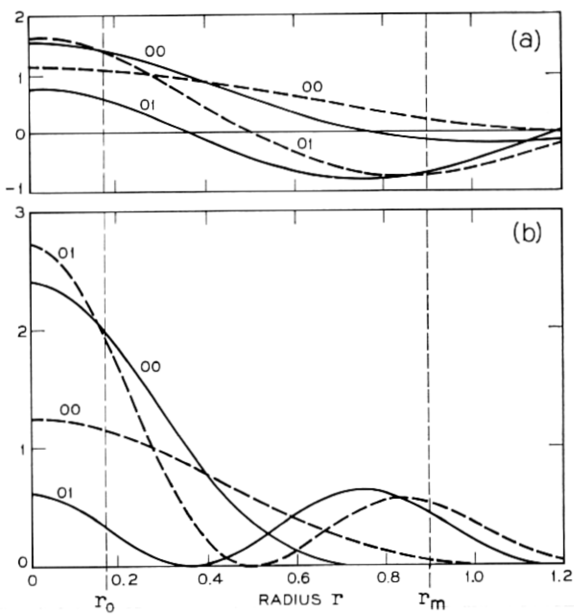

Fig. 7 — (a) Field amplitude $g_{lp}^{(j)}(r)$ and (b) field intensity $|g_{lp}^{(j)}(r)|^2$ for modes (lp) = (00) and (01) with $N_m = 0.8$ and $N_o = 0.03$. The dashed lines refer to mirror 1 (Fig. 1) and the solid lines to mirror 2. The radius of the aperture in mirror 1 is $r_o = 0.173$.

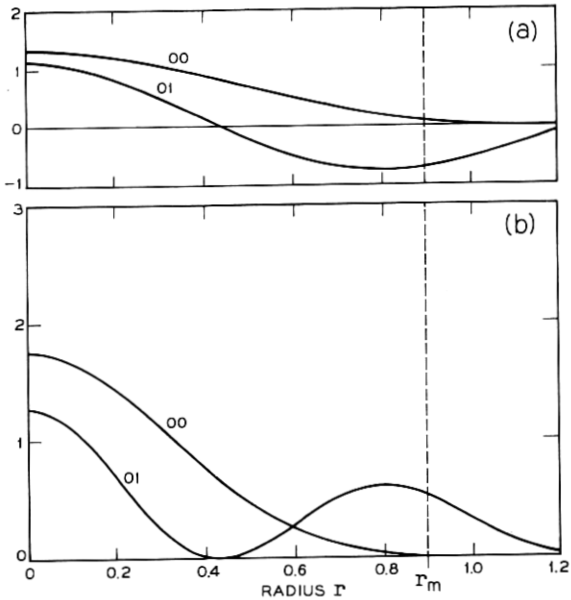

Fig. 8 — (a) Field amplitude $g_{lp}(r)$ and (b) field intensity $|g_{lp}(r)|^2$ for modes $(lp) = (00)$ and (01) with $N_m = 1.6$ and $N_o = 0$. The field distributions are identical on both mirrors.

$$\kappa_{lp}G_m^{(2)}(l, p)$$

$$= \sum_{k=1}^{M} \frac{(-1)^{k-1}(\pi N_m)^{l+m+k-1}}{[(m-1)!\,(m+l-1)!\,(k-1)!\,(k+l-1)!]^{\frac{1}{2}}(l+m+k-1)} G_k^{(1)}(l, p). \tag{22b}$$

We have used the definitions (5b) and (7) to replace (r_m^2, r_o^2) by the Fresnel numbers (N_m, N_o).

It is convenient to view $G_m^{(i)}(l, p)$ as the mth component of an M-dimensional vector $\mathbf{G}^{(i)}(l, p)$. We define $\mathbf{B}$ to be the $M \times M$ diagonal matrix with elements $B_{mm} = (-1)^{m-1}$. We also define real symmetric matrices $\mathbf{S}^{(1)}(l)$ and $\mathbf{S}^{(2)}(l)$ with elements

$$S_{mk}^{(1)}(l) = \frac{(\pi N_m)^{l+m+k-1}}{[(m-1)!\,(m+l-1)!\,(k-1)!\,(k+l-1)!]^{\frac{1}{2}}(l+m+k-1)}, \tag{23a}$$

$$S_{mk}^{(2)}(l) = \frac{[(\pi N_m)^{l+m+k-1} - (\pi N_o)^{l+m+k-1}]}{[(m-1)!\,(m+l-1)!\,(k-1)!\,(k+l-1)!]^{\frac{1}{2}}(l+m+k-1)}. \tag{23b}$$

With these definitions equations (22) can be written more compactly

$$\kappa_{lp}\mathbf{G}^{(1)}(l, p) = \mathbf{S}^{(2)}(l)\cdot\mathbf{B}\cdot\mathbf{G}^{(2)}(l, p), \tag{24a}$$

$$\kappa_{lp}\mathbf{G}^{(2)}(l, p) = \mathbf{S}^{(1)}(l)\cdot\mathbf{B}\cdot\mathbf{G}^{(1)}(l, p). \tag{24b}$$

Eliminating $\mathbf{G}^{(2)}$, we obtain

$$\kappa_{lp}^2\mathbf{G}^{(1)}(l, p) = \mathbf{S}^{(2)}(l)\cdot\mathbf{B}\cdot\mathbf{S}^{(1)}(l)\cdot\mathbf{B}\cdot\mathbf{G}^{(1)}(l, p), \tag{25}$$

which is a single M-dimensional matrix eigenvalue equation.

It is generally useful to transform equation (25) such that the matrix to be diagonalized is real symmetric (or Hermitian). Because $\mathbf{S}^{(2)}(l)$ is real symmetric with nonnegative eigenvalues, we can find a real lower-triangular matrix $\mathbf{P}(l)$ such that

$$\mathbf{S}^{(2)}(l) = \mathbf{P}(l)\cdot\mathbf{P}(l)^T. \tag{26}$$

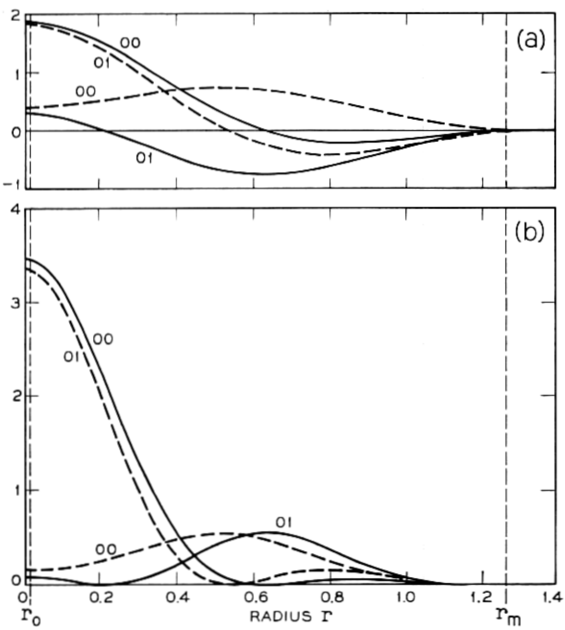

Fig. 9 — (a) Field amplitude $g_{lp}^{(j)}(r)$ and (b) field intensity $|g_{lp}^{(j)}(r)|^2$ for modes $(lp) = (00)$ and (01) with $N_m = 1.6$ and $N_o = 0.0001$. The dashed lines refer to mirror 1 (Fig. 1) and the solid lines to mirror 2. The radius of the aperture in mirror 1 is $r_o = 0.01$.

If we define a new vector

$$\mathbf{F}(l, p) = \mathbf{P}(l)^{-1} \cdot \mathbf{G}^{(1)}(l, p), \tag{27}$$

then (25) can be written

$$\kappa_{lp}^2 \mathbf{F}(l, p) = \mathbf{P}(l)^T \cdot \mathbf{B} \cdot \mathbf{S}^{(1)}(l) \cdot \mathbf{B} \cdot \mathbf{P}(l) \cdot \mathbf{F}, \tag{28}$$

for which the matrix on the right hand side is obviously real symmetric. If $\mathbf{U}(l)$ is the real orthogonal matrix which diagonalizes this matrix, then

$$\mathbf{U}(l) \cdot \mathbf{K}(l) = \mathbf{P}(l)^T \cdot \mathbf{B} \cdot \mathbf{S}^{(1)}(l) \cdot \mathbf{B} \cdot \mathbf{P}(l) \cdot \mathbf{U}(l) \tag{29}$$

where $\mathbf{K}(l)$ is diagonal with elements $K_{pp}(l) = \kappa_{lp}^2$, $p = 1$ to M. The eigenvector $\mathbf{F}(l, p)$ of (28) corresponds to the pth column of $\mathbf{U}(l)$ and, from (27),

$$\mathbf{G}^{(1)}(l, p) = \mathbf{P}(l) \cdot \mathbf{F}(l, p). \tag{30}$$

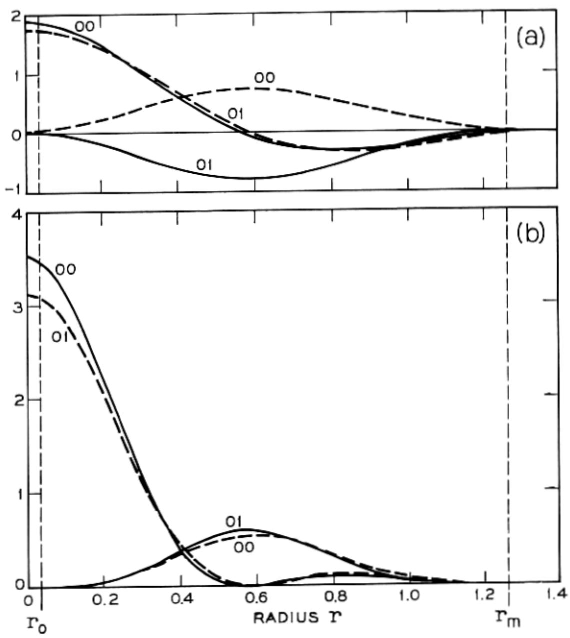

Fig. 10 — (a) Field amplitude $g_{lp}^{(J)}(r)$ and (b) field intensity $|g_{lp}^{(J)}(r)|^2$ for modes $(lp) = (00)$ and (01) with $N_m = 1.6$ and $N_o = 0.001$. The dashed lines refer to mirror 1 (Fig. 1) and the solid lines to mirror 2. The radius of the aperture in mirror 1 is $r_o = 0.0316$.

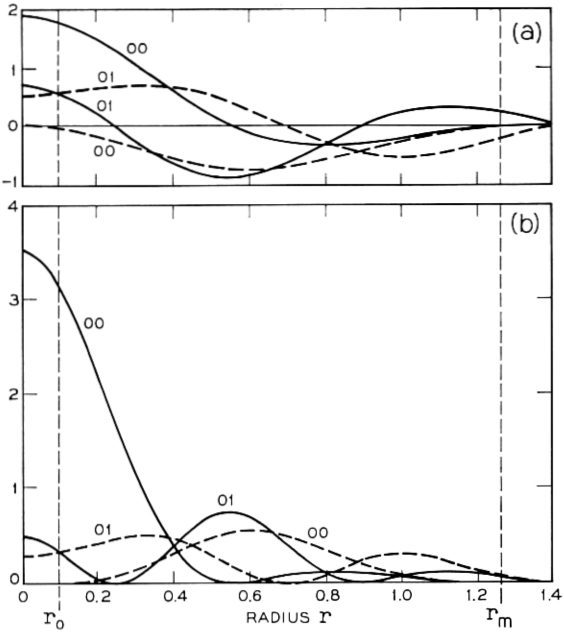

Fig. 11 — (a) Field amplitude $g_{lp}^{(j)}(r)$ and (b) field intensity $|g_{lp}^{(j)}(r)|^2$ for modes (lp) = (00) and (01) with $N_m = 1.6$ and $N_o = 0.01$. The dashed lines refer to mirror 1 (Fig. 1) and the solid lines to mirror 2. The radius of the aperture in mirror 1 is $r_o = 0.1$.

The elements of $\mathbf{U}(l)$ and $\mathbf{K}(l)$ are easily computed numerically; the vectors $\mathbf{G}^{(1)}(l, p)$ follow from (30); the vectors $\mathbf{G}^{(2)}(l, p)$ follow from (24b); and the amplitudes $g_{lp}^{(j)}(r)$ follow from (18b) and (20).

The program used to compute the results reported in this paper required a nominal 0.0003 hr. of GE 635 processor time to compute the M different eigenvalues $|\kappa_{lp}|$ and eigenvectors $[\mathbf{G}^{(1)}(l, p), \mathbf{G}^{(2)}(l, p)]$ for $M = 20$. Timing for other values of M varies roughly as M^3.

REFERENCES

1. McCumber, D. E., "Eigenmodes of a Symmetric Cylindrical Confocal Laser Resonator and their Perturbation by Output-Coupling Apertures," B.S.T.J., *44*, No. 2 (February 1965), pp. 333–363.
2. Patel, C. K. N., Faust, W. L., McFarlane, R. A., and Garrett, C. G. B., "Laser Action up to 57.355μ in Gaseous Discharges (Ne, He-Ne)," Appl. Phys. Letters, *4*, No. 1 (January 1, 1964), pp. 18–19.
3. Fox, A. G., and Li, T., "Resonant Modes in a Maser Interferometer," B.S.T.J., *40*, No. 2 (March 1961), pp. 453–488.

4. Boyd, G. D., and Kogelnik, H., "Generalized Confocal Resonator Theory," B.S.T.J., *41*, No. 4 (July 1962), pp. 1347–1369.
5. Kogelnik, H., "Modes in Optical Resonators," in *Lasers*, vol. 1, ed. A. K. Levine, New York: Marcel Dekker, Inc., 1966, pp. 295–347.
6. Gordon, J. P., and Kogelnik, H., "Equivalence Relations Among Spherical Mirror Optical Resonators," B.S.T.J., *43*, No. 6 (November 1964), pp. 2873–2886.
7. Goubau, G., and Schwering, F., "On the Guided Propagation of Electromagnetic Wave Beams," IRE Trans. Antennas Propagation, *AP-9*, No. 3 (May 1961), pp. 248–256.
8. Beyer, J. B., and Scheibe, E. H., "Higher Modes in Guided Electromagnetic-Wave Beams," IRE Trans. Antennas Propagation, *AP-10*, No. 3 (May 1962), pp. 349–350.
9. Slepian, D., "Prolate Spheroidal Wave Functions, Fourier Analysis and Uncertainty—IV: Extensions to Many Dimensions; Generalized Prolate Spheroidal Functions," B.S.T.J., *43*, No. 6 (November 1964), pp. 3009–3057.
10. Faust, W. L., unpublished work.